



## HIGH-ORDER THEORY OF MULTILAYER PLATES. THE IMPACT PROBLEM

A. N. SHUPIKOV,\* S. V. UGRIMOV, A. V. KOLODIAZHNY and  
V. G. YARESCHENKO

Institute for Problems in Machinery of the Ukrainian National Academy of Sciences,  
2/10 Pozharsky Street, Kharkov, 310046, Ukraine

(Received 4 June 1997; in revised form 12 December 1997)

**Abstract**—The high-order theory of multilayer plates is presented in this paper. The model is based on the hypothesis of the nonlinear dependence of displacements on the transverse coordinate in each layer. The strains in each layer are taken into account.

The feasibility of the theory is shown by example of the problem of a ball impacting a multilayer plate. The numerical results are compared with experimental data.

The suggested theory is also compared with the Timoshenko type theory. The advantage of the suggested model is demonstrated for the case of localized loads action. © 1998 Elsevier Science Ltd. All rights reserved.

### 1. INTRODUCTION

Multilayer plates are widely used in modern machine-building. This requires further refining of mathematical models describing their behavior. The selection of a model adequately describing the response of a structure is made on the basis of several criteria depending on the concrete problem. As a rule, the following criteria are used: relative plate thickness  $h/L$  ( $h$  is the plate thickness,  $L$  is the characteristic problem dimension), relationship of the layers elastic properties, type of loading (localization in space and time).

In the case of small relative thicknesses and distributed loads smoothly changing in time, a valid result may be obtained on the basis of the first-order theory (see, for example, Reissner, 1944; Reddy, 1989; Smetankina *et al.*, 1995). When calculating structures with a big relative thickness and heterogeneous layers affected by localized loads, high-order refined theories are used (e.g. Nelson and Lorch, 1974; Lo *et al.*, 1977b; Thangitham *et al.*, 1987; Reddy, 1990; Nosier *et al.*, 1994). These theories are based on the hypotheses of the nonlinear dependence of displacements on the transverse coordinate, and they take into account transverse strains. As a rule, these models are used for calculating structures under static loading (Lo *et al.*, 1977b).

In this paper, the model of a multilayer plate—HORT (High Order Refined Theory)—based on hypotheses for each layer has been suggested. The hypotheses for tangential displacements are presented by cubic dependencies on the transverse coordinate, and for normal displacements—a quadratic dependence. The suggested model is a generalization of the approach described by Lo *et al.* (1977a).

The feasibility of this theory is demonstrated by example of the problem of transient vibrations of a plate under the influence of a low-velocity impact. The contact between the indenter and the plate is described on the basis of Hertz's law. The possibility of using Hertz's law has been discussed in the fundamental works of Dinnik (1952), Timoshenko (1959), Goldsmith (1960), Kilchevsky (1976), Panovco (1977), Johnson (1987), Nosier *et al.* (1994). The analysis conducted by these authors convinces us that the use of Hertz's law is justified at elastic low-velocity impact.

The problem solution is presented in the form of trigonometric series. The numerical results are compared with experimental data. The experiment was carried out by using

\* Author to whom correspondence should be addressed.

dynamic wide-range strain measurement technique (see Vorobiev *et al.*, 1989). The technique ensures detection of the current time-dependent strain values and measurements of time intervals.

For the case of impulse loading, the suggested theory is compared with the first-order refined theory (FORT) proposed by Smetankina *et al.* (1995).

## 2. MULTILAYER PLATE

A multilayer plate consists of uniform isotropic constant thickness layers. The contact between the layers excludes their delamination and mutual slipping. The plate is considered in the Cartesian system of coordinates  $xyz$  connected with the external surface of the first layer (Fig. 1).

The theory describing the behavior of a plate under transient loading is based on the high-order accuracy hypotheses (Lo *et al.*, 1977a) for each of the layers.

To describe the displacement of a point in the  $i$ -th layer in the direction of the coordinate axes, the following kinematic relationships are used

$$\begin{aligned} u_i(x, y, z, t) &= u_0 + \sum_{k=1}^3 \left[ \sum_{j=1}^{i-1} h_j^k u_{jk} + (z - \delta_{i-1})^k u_{ik} \right]; \\ v_i(x, y, z, t) &= v_0 + \sum_{k=1}^3 \left[ \sum_{j=1}^{i-1} h_j^k v_{jk} + (z - \delta_{i-1})^k v_{ik} \right]; \\ w_i(x, y, z, t) &= w_0 + \sum_{l=1}^2 \left[ \sum_{j=1}^{i-1} h_j^l w_{jl} + (z - \delta_{i-1})^l w_{il} \right], \end{aligned} \quad (1)$$

where

$$h_j^k = (h_j)^k, \quad \delta_i = \sum_{j=1}^i h_j; \quad \delta_{i-1} \leq z \leq \delta_i; \quad i = \overline{1, I}.$$

Here  $t$  is time;  $h_i$  is the thickness of the  $i$ -th layer;  $I$  is the number of layers in a pack;  $u_0$ ,  $v_0$ ,  $w_0$ ,  $u_{jk}$ ,  $v_{jk}$ ,  $w_{jl}$  are the sought for functions depending on  $x$ ,  $y$ ,  $t$ .

The strains in the  $i$ -th layer are defined by Cauchy's law

$$\begin{aligned} \varepsilon_x^i &= u_{0,x} + \sum_{k=1}^3 \left[ \sum_{j=1}^{i-1} h_j^k u_{jk,x} + (z - \delta_{i-1})^k u_{ik,x} \right]; \\ \varepsilon_y^i &= v_{0,y} + \sum_{k=1}^3 \left[ \sum_{j=1}^{i-1} h_j^k v_{jk,y} + (z - \delta_{i-1})^k v_{ik,y} \right]; \\ \varepsilon_z^i &= w_{i1} + 2(z - \delta_{i-1})w_{i2}; \end{aligned}$$

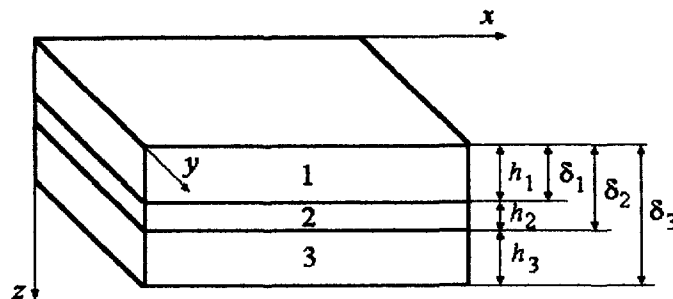


Fig. 1. Multilayer plate.

$$\begin{aligned}
 \gamma_{xy}^i &= \gamma_{yx}^i = u_{0,y} + v_{0,x} + \sum_{k=1}^3 \left[ \sum_{j=1}^{i-1} h_j^k (u_{jk,y} + v_{jk,x}) + (z - \delta_{i-1})^k (u_{ik,y} + v_{ik,x}) \right]; \\
 \gamma_{xz}^i &= \gamma_{zx}^i = u_{i1} + 2(z - \delta_{i-1})u_{i2} + 3(z - \delta_{i-1})^2 u_{i3} \\
 &\quad + w_{0,x} + \sum_{l=1}^2 \left[ \sum_{j=1}^{i-1} h_j^l w_{jl,x} + (z - \delta_{i-1})^l w_{il,x} \right]; \\
 \gamma_{yz}^i &= \gamma_{zy}^i = v_{i1} + 2(z - \delta_{i-1})v_{i2} + 3(z - \delta_{i-1})^2 v_{i3} \\
 &\quad + w_{0,y} + \sum_{l=1}^2 \left[ \sum_{j=1}^{i-1} h_j^l w_{jl,y} + (z - \delta_{i-1})^l w_{il,y} \right].
 \end{aligned} \tag{2}$$

Based on Hooke’s law, the relationship between the stresses and the strains in the  $i$ -th layer is established

$$\begin{aligned}
 \sigma_x^i &= \frac{E_i}{1 + \nu_i} \left( \varepsilon_x^i + \frac{\nu_i}{1 - 2\nu_i} \theta_i \right); \quad \sigma_y^i = \frac{E_i}{1 + \nu_i} \left( \varepsilon_y^i + \frac{\nu_i}{1 - 2\nu_i} \theta_i \right); \\
 \sigma_z^i &= \frac{E_i}{1 + \nu_i} \left( \varepsilon_z^i + \frac{\nu_i}{1 - 2\nu_i} \theta_i \right); \\
 \tau_{xy}^i &= \frac{E_i}{2(1 + \nu_i)} \gamma_{xy}^i; \quad \tau_{xz}^i = \frac{E_i}{2(1 + \nu_i)} \gamma_{xz}^i; \quad \tau_{yz}^i = \frac{E_i}{2(1 + \nu_i)} \gamma_{yz}^i;
 \end{aligned} \tag{3}$$

where  $\theta_i = \varepsilon_x^i + \varepsilon_y^i + \varepsilon_z^i$  is the relative volume change.

The equations of motion of a multilayer plate and the natural boundary conditions are obtained for Hamilton’s variation principle

$$\int_{t_0}^{t_1} (\delta K - \delta \Pi + \delta' F) dt = 0. \tag{4}$$

Here  $\delta K$ ,  $\delta \Pi$  are the variations of kinetic and potential energy,  $\delta' F$  is the elementary work of external forces.

We consider a rectangular plate limited by the coordinate lines  $x = 0$ ,  $x = A$ ,  $y = 0$ ,  $y = B$ . In this case the kinetic energy may be presented in the form

$$K = \frac{1}{2} \sum_{i=1}^I \rho_i \int_0^A \int_0^B \int_{\delta_{i-1}}^{\delta_i} (\dot{u}_i^2 + \dot{v}_i^2 + \dot{w}_i^2) dx dy dz.$$

Here  $\rho_i$  is the density of the  $i$ -th layer, symbol  $(\dot{\cdot})$  designates the derivative  $\partial/\partial t$ .

The potential energy of the plate is defined as follows :

$$\Pi = \frac{1}{2} \sum_{i=1}^I \int_0^A \int_0^B \int_{\delta_{i-1}}^{\delta_i} (\sigma_x^i \varepsilon_x^i + \sigma_y^i \varepsilon_y^i + \sigma_z^i \varepsilon_z^i + \tau_{xy}^i \gamma_{xy}^i + \tau_{xz}^i \gamma_{xz}^i + \tau_{yz}^i \gamma_{yz}^i) dx dy dz.$$

In the case when the external load is applied to the external surface of the first layer ( $z = 0$ ) the elementary work of the external forces may be presented as :

$$\delta' F = \int_0^A \int_0^B (q_x \delta u_0 + q_y \delta v_0 + q_z \delta w_0) dx dy dz,$$

where  $q_x, q_y, q_z$  are the coordinate axes projections of external force applied to the external surface of the first layer.

In the matrix form the equation obtained have the following form :

$$\Omega \ddot{\mathbf{U}} - \Lambda \mathbf{U} = \mathbf{Q}. \quad (5)$$

Here  $\mathbf{U}$  is a vector whose components are the sought for functions

$$\mathbf{U} = (u_0, v_0, w_0, u_{ik}, v_{ik}, w_{il})^T, \quad i = \overline{1, I}, \quad k = 1, 2, 3, \quad l = 1, 2.$$

$\Lambda, \Omega$  are symmetric matrices with the dimensions  $(8I+3) \times (8I+3)$ . Therefore, in Appendix 1 their elements are given only for the lower triangle.

Vector  $\mathbf{Q}$  is of the dimension  $(8I+3)$  and its elements have the following form

$$\mathbf{Q} = (q_x, q_y, q_z, 0, \dots, 0)^T.$$

The boundary conditions for the case of simply supported rectangular plate  $A \times B$  are given in Appendix 2.

### 3. METHOD OF SOLVING THE SYSTEM OF EQUATIONS

The sought for functions  $u_0, v_0, w_0, u_{ik}, v_{ik}, w_{il}$  ( $i = \overline{1, I}, k = 1, 2, 3, l = 1, 2$ ) and the external load  $q_x, q_y, q_z$  are expanded into trigonometric series by functions satisfying the boundary conditions

$$\begin{aligned} [u_0(x, y, t), u_{ik}(x, y, t), q_x(x, y, t)] &= \sum_{m=1}^{\infty} \sum_{n=1}^{\infty} [\Phi_{0mn}^x(t), \Phi_{ikmn}^x(t), q_{xmn}(t)] B_{1mn}(x, y); \\ [v_0(x, y, t), v_{ik}(x, y, t), q_y(x, y, t)] &= \sum_{m=1}^{\infty} \sum_{n=1}^{\infty} [\Phi_{0mn}^y(t), \Phi_{ikmn}^y(t), q_{ymn}(t)] B_{2mn}(x, y); \\ [w_0(x, y, t), w_{il}(x, y, t), q_z(x, y, t)] &= \sum_{m=1}^{\infty} \sum_{n=1}^{\infty} [\Phi_{0mn}^z(t), \Phi_{ilmn}^z(t), q_{zmn}(t)] B_{3mn}(x, y), \\ i &= \overline{1, I}, \quad k = 1, 2, 3, \quad l = 1, 2. \end{aligned} \quad (6)$$

Functions  $B_{kmn}(x, y)$ ,  $k = 1, 2, 3$  in the case of simple supported plate take the form

$$\begin{aligned} B_{1mn}(x, y) &= \cos \frac{m\pi}{A} x \cdot \sin \frac{n\pi}{B} y; \quad B_{2mn}(x, y) = \sin \frac{m\pi}{A} x \cdot \cos \frac{n\pi}{B} y; \\ B_{3mn}(x, y) &= \sin \frac{m\pi}{A} x \cdot \sin \frac{n\pi}{B} y. \end{aligned}$$

As a result, the problem of transient vibrations of a multilayer plate for each pair of values  $m$  and  $n$  is reduced to integration of a system of ordinary differential equations with constant coefficients

$$\Omega \ddot{\Phi}^{mn} - \Lambda^{mn} \Phi^{mn} = \mathbf{q}^{mn}, \quad (7)$$

where  $\Phi^{mn}$  and  $\mathbf{q}^{mn}$  are vectors with the following components

$$\Phi^{mn} = (\Phi_{0mn}^x, \Phi_{0mn}^y, \Phi_{0mn}^z, \Phi_{ikmn}^x, \Phi_{ikmn}^y, \Phi_{ikmn}^z)^T, \quad i = \overline{1, I}, \quad k = 1, 2, 3,$$

$$\mathbf{q}^{mn} = (q_{xmn}, q_{ymn}, q_{zmn}, 0, \dots, 0)^T.$$

Matrix  $\Lambda^{mn}$  is obtained from  $\Lambda$  by substituting the partial derivatives in the expressions for the matrix elements with coefficients yielded during differentiation of coordinate functions. Equations (7) are integrated by the modified method of expanding the solution into Taylor's series. The displacements are defined according to formulas (1), (6), and the stresses are defined by (2), (3).

#### 4. IMPACT

The plate being investigated is located horizontally. The indenter (a cylinder with a hemispheric butt end of radius  $R$ ) is dropped from the height  $h$  and at the moment of impact it has the velocity  $V_0 = \sqrt{2gh}$ , where  $g$  is the gravitational acceleration.

When solving the impact problem, the system of eqns (5) is to be complemented with the ball motion equation and the condition of motion consistency of the indenter and the plate.

The indenter equation of motion and the initial conditions have the form :

$$M\ddot{z} = Mg - P, \quad z(0) = 0, \quad \dot{z}(0) = V_0.$$

Here  $M$  is the ball mass;  $z = z(t)$  and  $P$  is the contact force.

The consistency condition is based on the hypothesis that full displacement of the indenter in the process of impact consists of the plate dynamic deflection and indentation in the contact point :

$$z - w_0 - \alpha = 0,$$

where  $\alpha$  is the indentation.

The indentation  $\alpha$  is accounted for by solving Hertz's problem on the indentation of a ball into an elastic semispace (see Dinnik, 1952) :

$$\alpha = kP^{2/3};$$

$$k = \left[ \frac{9}{256} \frac{(\theta_1 + \theta)}{R} \right]^{1/3};$$

$$\theta_1 = \frac{4(1 - \nu_1)}{E_1}, \quad \theta = \frac{4(1 - \nu)}{E}.$$

Here  $E, \nu$  are Young's indenter material;  $E_1, \nu_1$  are similar characteristics for the plate first layer.

It is assumed that the contact pressure is distributed over a circular area with the radius  $a(t)$  according to the law

$$q(x, y, t) = P_0(t) \left[ 1 - \frac{(x - x_0)^2 + (y - y_0)^2}{a(t)^2} \right]^{1/2},$$

where  $x_0, y_0$  are the coordinates of the contact point. Function  $q(x, y, t)$  shall satisfy the condition :

$$P = \iint_S q \, dS = \frac{2}{3} P_0 \pi a^2,$$

yielding

$$P_0 = \frac{3}{2} \frac{P}{\pi a^2}.$$

The value  $a(t)$  is computed from the formula

$$a(t) = \left[ \frac{3}{16} P(t) (\theta + \theta_1) \right]^{1/3}.$$

The Fourier series expansion coefficients  $q(x, y, t)$  have the form

$$q_{mn} = \frac{12P}{AB\rho_{mn}^2} \left[ \frac{\sin \rho_{mn}}{\rho_{mn}} - \cos \rho_{mn} \right] \sin \frac{m\pi x_0}{A} \sin \frac{n\pi y_0}{B}, \quad \text{where } \rho_{mn} = \pi a \sqrt{\frac{m^2}{A^2} + \frac{n^2}{B^2}}.$$

## 5. EXPERIMENTAL TECHNIQUE

To measure the plate strain under an impact action, the method of dynamic wide-range strain measurement was used. The plate fastening over its periphery simulates the condition of simple supporting. Loading is effected by dropping an indenter onto the plate from a specified height.

A three-component rosette of strain gauges was bonded onto the middle of the plate on the external surface of the last layer. In this work we used small-base (measurement base—1 mm) foil piezoresistors. A piezoceramic accelerometer located on the external surface of the first layer at a distance of 3 cm from the impact point was used as a triggering transmitter.

A bridge circuit is used for measuring the strain. Prior to the experiment, balancing and calibration of the measurement channels was performed.

The signals from the strain gauge rosette were input to the piezoamplifier, and then to the computerized measuring-and-computing system which recorded and processed the data obtained.

The more detail description of experimental method have been presented in the work by Smetankina *et al.* (1995).

## 6. RESULT

Investigated were simple supported plates. The values of the mechanical parameters of the materials being used are given in Table 1.

A single-layer plate has the following geometric parameters:  $A = 0.47$  m;  $B = 0.42$  m;  $h = 26$  mm. The plate was made of silica glass.

The three-layer plate has the following geometric parameters:  $A = 0.47$  m;  $B = 0.42$  m;  $h_1 = h_3 = 12$  mm;  $h_2 = 2$  mm. The carrier layers ( $i = 1, 3$ ) are made of silica glass and the adhesive layer ( $i = 2$ ) is made of a polymer.

Table 1. Characteristics of the layer materials

Material	$E$ [MPa]	$\nu$	$\rho$ [kg m <sup>-3</sup> ]
Silica glass	$6.67 \times 10^4$	0.22	$2.5 \times 10^3$
Organic glass	$5.59 \times 10^3$	0.38	$1.2 \times 10^3$
Polymer	$2.74 \times 10^2$	0.38	$1.2 \times 10^3$

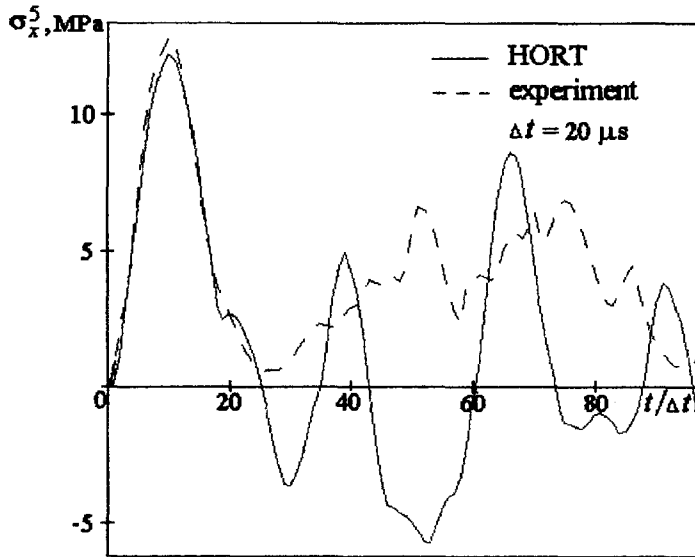


Fig. 2. Stresses in a five-layer plate at an impact. Indenter no. 1,  $h = 1$  m.

Similar characteristics for a five-layer plate have the following values:  $A = 0.6$  m;  $B = 0.28$  m;  $h_1 = 5$  mm;  $h_2 = 3$  mm;  $h_3 = 15$  mm;  $h_4 = 2$  mm;  $h_5 = 20$  mm. The carrier layers ( $i = 1, 3, 5$ ) are made of silica glass and the adhesive ones ( $i = 2, 4$ ) are made of polymer.

The plate response to impulse and impact loading has been investigated.

Impact loading was effected by two indenters: no. 1 and no. 2 ( $R_1 = R_2 = 30$  mm). The indenters were made of organic glass, and their masses were  $M_1 = 0.215$  kg and  $M_2 = 0.120$  kg, respectively. The mechanical characteristics of organic glass are presented in Table 1.

In all the investigated cases the impact was made on the external surface of the first layer in the middle of the plate. The stresses are calculated for the external surface of the last layer in the impact point.

Figure 2 shows the dynamic response of a five-layer plate to the action of indenter no. 1 dropped from the height  $h = 1$  m (solid line). In the same figure, similar results obtained experimentally (dashed line) are shown.

Figure 3 shows the numerical values of flexures of the external surfaces of the first (solid line) and last (dashed line) layers in the impact point.

Similar results for a three-layer plate and indenter no. 2 are shown in Figs 4 and 5.

Figure 6 shows the dependence of the maximal values of normal stresses in a three-layer plate on the height of dropping of indenter no. 2. The solid line designates the numerical result and the dashed line shows the experimental one.

The response of a multilayer plate to impulse load action has also been investigated.

The impulse load is applied to a rectangular area  $x_1 \leq x \leq x_2$ ,  $y_1 \leq y \leq y_2$  according to the law

$$q_x = q_y = 0, \quad q_z = P_0 H(t),$$

where  $P_0$  is the load intensity and  $H(t)$  is Heaviside's function.

In this case, the total force applied to the plate is expressed by

$$P = \int_{x_1}^{x_2} \int_{y_1}^{y_2} q_z \, dx \, dy = P_0 (x_2 - x_1) (y_2 - y_1).$$

The value  $P_0$  is selected so that the total force value be equal  $P = 2$  kN in all the cases being investigated.

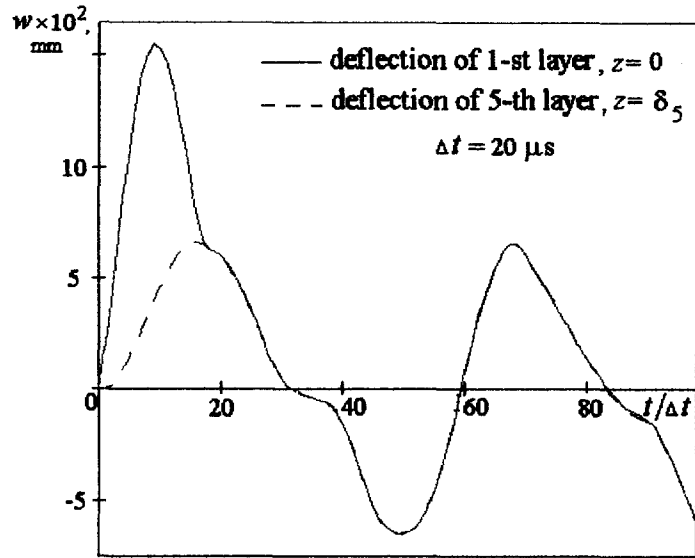


Fig. 3. Deflections of external surfaces of a 5-layer plate. Indenter no. 1,  $h = 1$  m.

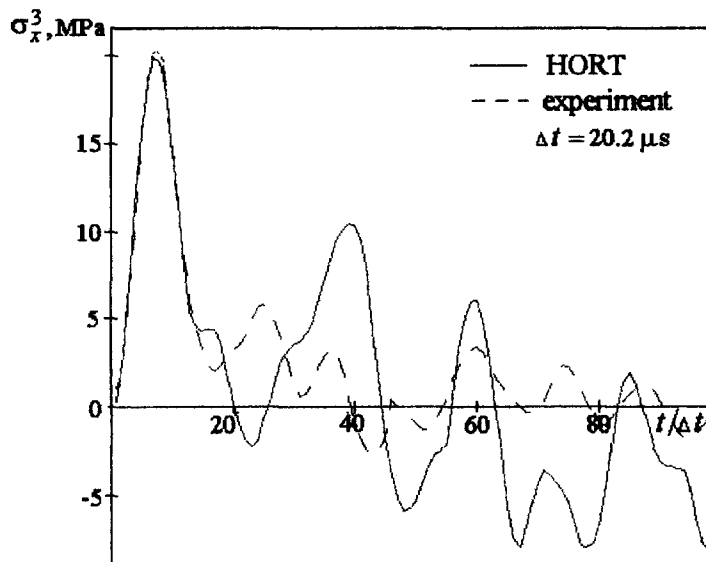


Fig. 4. Stresses in a three-layer plate at an impact. Indenter no. 2,  $h = 1$  m.

Figure 7 shows the distribution of the normal stresses over the thickness in the center of a single-layer plate at the moment of time when they reach their maximum values. The impulse load is evenly distributed over the external surface of the first layer. The load intensity  $P_0 = 10.13$  kPa.

Figure 8 shows similar results for the case when the impulse load is evenly distributed over a square with the side 5 mm in the middle of the plate. The load intensity  $P_0 = 80$  MPa.

Figures 9 and 10 show similar results for a three-layer plate. In this case the stresses in the carrier layers ( $i = 1, 3$ ) significantly exceed the stresses in the adhesive layer ( $i = 2$ ). Therefore their pictorial presentation in the accepted scale is difficult.



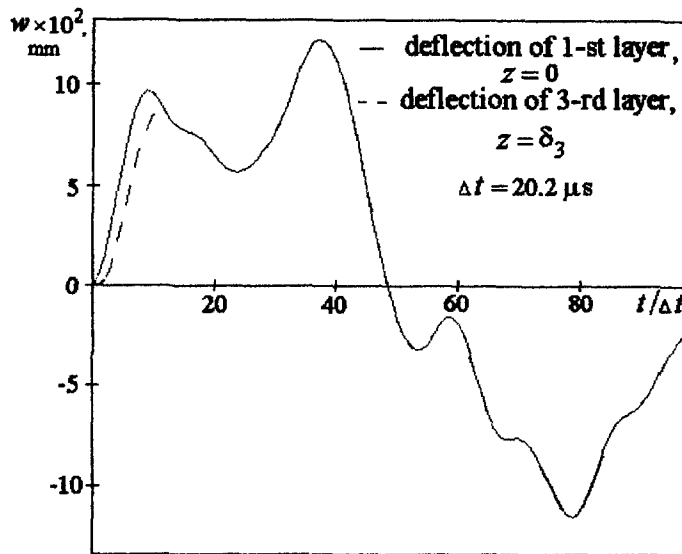


Fig. 5. Deflections of external surfaces of a three-layer plate. Indenter no. 2,  $h = 1$  m.

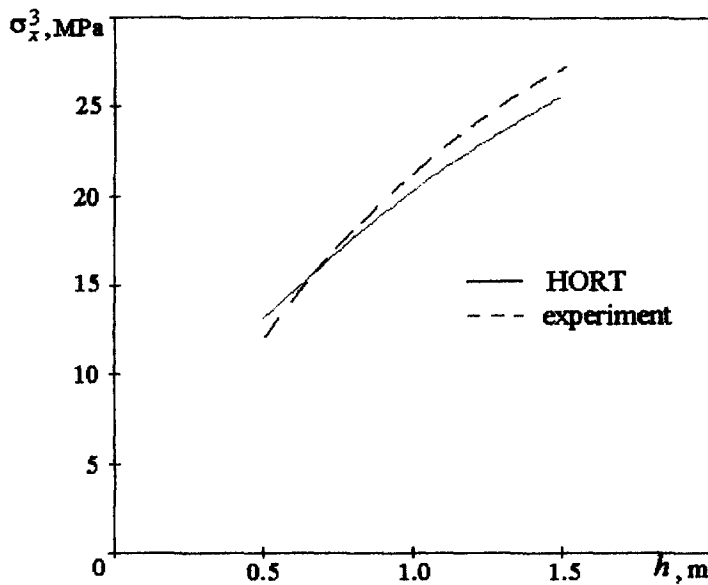


Fig. 6. Maximal stresses vs dropping height. Three-layer plate, indenter no. 2.

## 7. DISCUSSION

The theory of the multilayer plates proposed (HORT) is based on the kinetic hypothesis (1), which allows to take account of the effect of all the components of the stress tensor (3) and as a consequence, the effects of normal flexure and its strain in the transverse direction in each of its layers.

Comparison of theoretical and experimental data given in Figs 2, 4 and 6 indicates that the suggested theory consistently describes the process of transient strain of multilayer plates under impact loading.

In some cases (Fig. 3) of essential account is the normal strain in the transverse direction.

A good match of results obtained on the basis of theory FORT and the suggested theory HORT in the case of distributed loads (Figs 7 and 9).

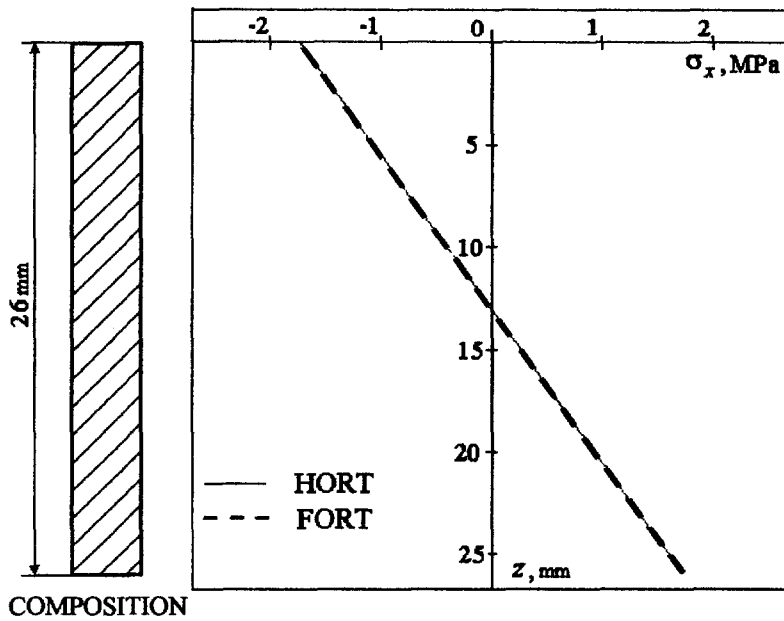


Fig. 7. Distribution of normal stresses over the thickness during deflection of a one-layer plate. Evenly distributed load.

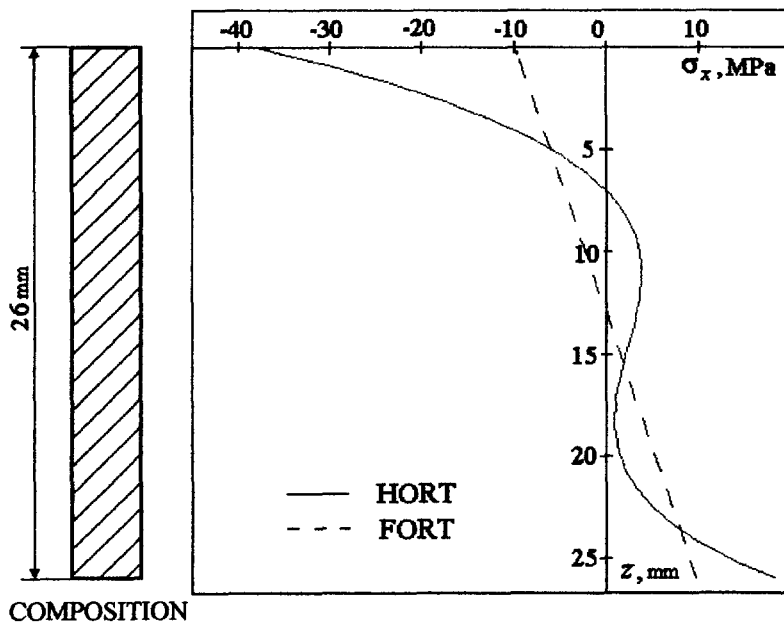


Fig. 8. Distribution of normal stresses over the thickness during deflection of a one-layer plate. Locally distributed load.

When localized loads act upon the plate the results differ drastically (Figs 8 and 10). This is due to the fact that the deformed state of a plate in the load zone is of an essentially 3-D character. In this case the stress distribution over the plate thickness is a nonlinear one.

The results presented demonstrate the advantage of this theory HORT when investigating the response of a structure under local actions, especially during impacts.

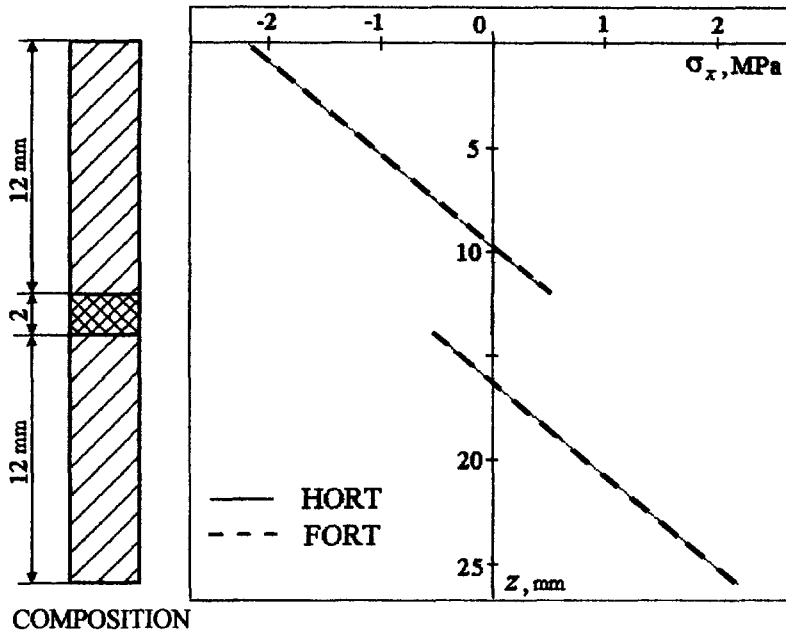


Fig. 9. Distribution of normal stresses over the thickness during deflection of a three-layer plate. Evenly distributed load.

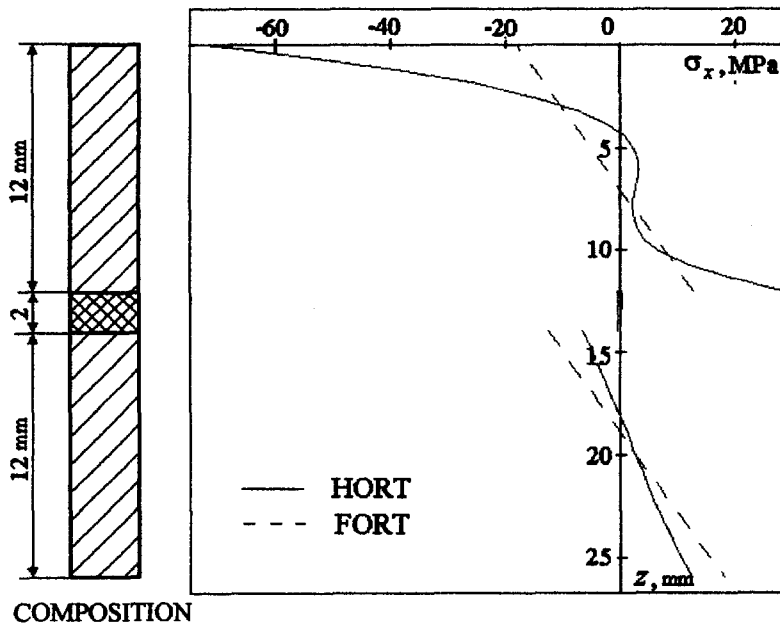


Fig. 10. Distribution of normal stresses over the thickness during deflection of a three-layer plate. Locally distributed load.

The suggested theory has a high-order approximation and its numerical implementation is associated with significant difficulties. Therefore, the researcher has to define cases where this application is justified. A detailed discussion of these issues is given in Lo *et al.* (1977a, b).

REFERENCES

Dinnik, A. N. (1952) *Selected Works*, Vol. 1. Academy of Sciences of the Ukrainian SSR Publishers, Kiev.  
 Goldsmith, W. (1960) *Impact. The Theory and Physical Behaviour of Colliding Solids*. Edward Arnold Publishers, London.

- Johnson, K. L. (1987) *Contact Mechanics*. Cambridge University Press, Cambridge.
- Kilchevsky, N. A. (1976) *Dynamic Contact Compression of Elastic Bodies*. Naukova Dumka, Kiev.
- Lo, K. H., Christensen, R. M. and Wu, E. M. (1977a) A high-order theory of plate deformation. Part 1: Homogeneous plates. *ASME Journal of Applied Mechanics* **44**, 663–668.
- Lo, K. H., Christensen, R. M. and Wu, E. M. (1977b) A high-order theory of plate deformation. Part 2: Laminated plates. *ASME Journal of Applied Mechanics* **44**, 669–676.
- Nelson, R. B. and Lorch, D. R. (1974) A refined theory of laminated orthotropic plates. *ASME Journal of Applied Mechanics* **41**, 177–183.
- Nosier, A., Kapania, R. K. and Reddy, J. N. (1994) Low-velocity impact of laminated composites using a layerwise theory. *Comput. Mech.*, **13**, 360–379.
- Panovco, Ja. G. (1977) *Introduction to the Theory of Mechanical Impact*. Nauka, Moskva.
- Reddy, J. N. (1989) On the generalization of displacement based laminate theories. *Applied Mechanics Review* **42**, S213–S222.
- Reddy, J. N. (1990) A general third-order nonlinear theory of plates with moderate thickness. *Int. J. Non-Lin. Mech.* **25**(6), 677–686.
- Reissner, E. (1944) On the theory of bending of elastic plates. *Journal of Mathematics and Physics* **23**, 184–191.
- Smetankina, N. V., Sotrikhin, S. Yu. and Shupikov, A. N. (1995) Theoretical and experimental investigation of vibration of multilayer plates under the action of impulse and impact loads. *International Journal of Solids and Structures* **32**, 1247–1258.
- Thangjitham, S., Librescu, L. and Cederbaum, G. (1987) Low-velocity impact response of orthotropic plates using a higher-order theory. *Proceedings of the 28th AIAA/ASME/ASCE/AHS/ASC Structures, Structural Dynamics and Material Conference*, pp. 448–457.
- Timoshenko, S. P. (1959) *Vibrations in Engineering*. Fizmatgiz, Moskva.
- Vorobiev, Yu. S., Kolodyazhny, A. V., Sevryukov, V. I. and Yanyutin, E. G. (1989) *Rapid Strain of Structural Elements*. Naukova Dumka, Kiev.

#### APPENDIX 1: ELEMENTS OF MATRICES $\Lambda$ , $\Omega$

Matrix  $\Lambda$ :

$$\begin{aligned} \Lambda_{1,1} &= C_{11} \frac{\partial^2}{\partial x^2} + C_{21} \frac{\partial^2}{\partial y^2}; \quad \Lambda_{2,1} = C_{31} \frac{\partial^2}{\partial x \partial y}; \quad \Lambda_{2,2} = C_{21} \frac{\partial^2}{\partial x^2} + C_{11} \frac{\partial^2}{\partial y^2}; \\ \Lambda_{3,1} &= \Lambda_{3,2} = 0; \quad \Lambda_{3,3} = -C_{21} \left( \frac{\partial^2}{\partial x^2} + \frac{\partial^2}{\partial y^2} \right); \quad \Lambda_{3+i+(k-1)l,1} = h_i^k \left( D_{1ik} \frac{\partial^2}{\partial x^2} + D_{2ik} \frac{\partial^2}{\partial y^2} \right); \\ \Lambda_{3+i+(k-1)l,2} &= \Lambda_{3+3l+i+(k-1)l,1} = h_i^k D_{3ik} \frac{\partial^2}{\partial x \partial y}; \quad \Lambda_{3+i+(k-1)l,3} = -h_i^k \beta_{2i} \frac{\partial}{\partial x}; \\ \Lambda_{3+i+(k-1)l,3+j+(r-1)l} &= \eta_{1ikr} \frac{\partial^2}{\partial x^2} + \eta_{2ikr} \frac{\partial^2}{\partial y^2} + \chi_{2ikr}; \\ \Lambda_{3+3l+i+(k-1)l,2} &= h_i^k \left( D_{2ik} \frac{\partial^2}{\partial x^2} + D_{1ik} \frac{\partial^2}{\partial y^2} \right); \quad \Lambda_{3+3l+i+(k-1)l,3} = -h_i^k \beta_{2i} \frac{\partial}{\partial y}; \\ \Lambda_{3+3l+i+(k-1)l,3+j+(r-1)l} &= \eta_{3ikr} \frac{\partial^2}{\partial x \partial y}; \quad \Lambda_{3+6l+i+(p-1)l,1} = h_i^p \beta_{4i} \frac{\partial}{\partial x}; \\ \Lambda_{3+3l+i+(k-1)l,3+3l+j+(r-1)l} &= \eta_{2ikr} \frac{\partial^2}{\partial x^2} + \eta_{1ikr} \frac{\partial^2}{\partial y^2} + \chi_{2ikr}; \\ \Lambda_{3+6l+i+(p-1)l,2} &= h_i^p \beta_{4i} \frac{\partial}{\partial y}; \quad \Lambda_{3+6l+i+(p-1)l,3} = -h_i^p D_{2ip} \left( \frac{\partial^2}{\partial x^2} + \frac{\partial^2}{\partial y^2} \right); \\ \Lambda_{3+6l+i+(p-1)l,3+j+(r-1)l} &= \zeta_{ikjr} \frac{\partial}{\partial x}; \quad \Lambda_{3+6l+i+(p-1)l,3+3l+j+(r-1)l} = \zeta_{ikjr} \frac{\partial}{\partial y}; \\ \Lambda_{3+6l+i+(p-1)l,3+6l+j+(l-1)l} &= -\eta_{2ipj} \left( \frac{\partial^2}{\partial x^2} + \frac{\partial^2}{\partial y^2} \right) + \chi_{1ipj}. \end{aligned}$$

Here

$$\begin{aligned} C_{\alpha i} &= \sum_{j=1}^l h_j \beta_{\alpha j}; \quad D_{\alpha i s} = C_{\alpha i+1} + \frac{h_i \beta_{\alpha i}}{s+1}; \\ \beta_{1i} &= \frac{E_i(1-\nu_i)}{(1+\nu_i)(1-2\nu_i)}; \quad \beta_{2i} = \frac{E_i}{2(1+\nu_i)}; \quad \beta_{3i} = \frac{E_i}{2(1+\nu_i)(1-2\nu_i)}; \quad \beta_{4i} = \frac{E_i \nu_i}{(1+\nu_i)(1-2\nu_i)}; \end{aligned}$$

$$\eta_{aikjr} = h_i^k h_j^r \begin{cases} D_{aik}, & j < i \\ D_{aik+r}, & j = i \\ D_{ajr}, & j > i \end{cases}; \quad \chi_{aikjr} = \begin{cases} 0, & j < i \\ -h_i^{k+r-1} \frac{kr\beta_{ai}}{k+r-1}, & j = i \\ 0, & j < i \end{cases}; \quad \zeta_{ikjr} = h_i^l h_j^r \begin{cases} \beta_{4i}, & j < i \\ \frac{\beta_{4i}p - \beta_{2i}r}{r+p}, & j = i \\ -\beta_{2j}, & j > i \end{cases},$$

where  $i, j = \overline{1, I}, k, r = 1, 2, 3, l, p = 1, 2$ .

Matrix  $\Omega$ :

$$\Omega_{1,1} = \Omega_{2,2} = -\Omega_{3,3} = \xi_1; \quad \Omega_{3+i+(k-1)l,1} = \Omega_{3+3l+i+(k-1)l,2} = h_i^k S_{ik}; \quad \Omega_{3+6l+i+(p-1)l,3} = -h_i^p S_{ip};$$

$$\Omega_{3+i+(k-1)l,3+j+(r-1)l} = \Omega_{3+3l+i+(k-1)l,3+3l+j+(r-1)l} = h_i^k h_j^r \begin{cases} S_{ik}, & j < i \\ S_{ik+r}, & j = i \\ S_{jr}, & j > i \end{cases};$$

$$\Omega_{3+6l+i+(p-1)l,3+6l+j+(l-1)l} = -h_i^p h_j^l \begin{cases} S_{ip}, & j < i \\ S_{ip+l}, & j = i \\ S_{jp}, & j > i \end{cases}$$

where

$$\xi_n = \sum_{i=n}^I h_i \rho_i; \quad S_{ik} = \xi_{i+1} + \frac{h_i \rho_i}{k+1}, \quad i, j = \overline{1, I}, \quad k, r = 1, 2, 3, \quad l, p = 1, 2.$$

The remaining matrix elements are equal to zero.

### APPENDIX 2: BOUNDARY CONDITIONS

The boundary conditions on the boundaries  $x = 0$  and  $x = A$  may be written in the following form:

$$[B_{i,j}^x]U = 0, \quad i, j = \overline{1, 8I+3}.$$

The corresponding conditions for the boundaries  $y = 0, y = B$  are of the form:

$$[B_{i,j}^y]U = 0, \quad i, j = \overline{1, 8I+3}.$$

Here

$$B_{1,1}^x = C_{11} \frac{\partial}{\partial x}; \quad B_{1,2}^x = C_{41} \frac{\partial}{\partial y}; \quad B_{1,3+j+(r-1)l}^x = h_j^r D_{1jr} \frac{\partial}{\partial x}; \quad B_{1,3+3l+j+(r-1)l}^x = h_j^r D_{4jr} \frac{\partial}{\partial y};$$

$$B_{1,3+6l+j+(l-1)l}^x = h_j^l \beta_{4j}; \quad B_{2,2}^x = B_{3,3}^x = B_{3+3l+i+(k-1)l,3+3l+i+(k-1)l}^x = B_{3+6l+i+(p-1)l,3+6l+i+(p-1)l}^x = 1;$$

$$B_{3+i+(k-1)l,1}^x = h_i^k D_{1ik} \frac{\partial}{\partial x}; \quad B_{3+i+(k-1)l,2}^x = h_i^k D_{4ik} \frac{\partial}{\partial y};$$

$$B_{3+i+(k-1)l,3+j+(r-1)l}^x = \eta_{1ikjr} \frac{\partial}{\partial x}; \quad B_{3+i+(k-1)l,3+3l+j+(r-1)l}^x = \eta_{4ikjr} \frac{\partial}{\partial y};$$

$$B_{3+i+(k-1)l,3+6l+j+(l-1)l}^x = h_i^k h_j^l \beta_{4j} \begin{cases} 0, & j < i \\ \frac{l}{k+l}, & j = i \\ 1, & j > i \end{cases};$$

$$B_{1,1}^y = B_{3,3}^y = B_{3+i+(k-1)l,3+i+(k-1)l}^y = B_{3+6l+i+(p-1)l,3+6l+i+(p-1)l}^y = 1;$$

$$B_{2,1}^y = C_{41} \frac{\partial}{\partial x}; \quad B_{2,2}^y = C_{11} \frac{\partial}{\partial y}; \quad B_{2,3+j+(r-1)l}^y = h_j^r D_{4jr} \frac{\partial}{\partial x}; \quad B_{2,3+3l+j+(r-1)l}^y = h_j^r D_{1jr} \frac{\partial}{\partial y};$$

$$B_{2,3+6l+j+(l-1)l}^y = h_j^l \beta_{4j}; \quad B_{3+3l+i+(k-1)l,1}^y = h_i^k D_{4ik} \frac{\partial}{\partial x}; \quad B_{3+3l+i+(k-1)l,2}^y = h_i^k D_{1ik} \frac{\partial}{\partial y};$$

$$B_{3+3l+i+(k-1)l,3+j+(r-1)l}^y = \eta_{4ikjr} \frac{\partial}{\partial x}; \quad B_{3+3l+i+(k-1)l,3+3l+j+(r-1)l}^y = \eta_{1ikjr} \frac{\partial}{\partial y};$$

$$B_{3+3l+i+(k-1)l,3+6l+j+(l-1)l}^y = h_i^k h_j^l \beta_{4j} \begin{cases} 0, & j < i \\ \frac{l}{k+l}, & j = i \\ 1, & j > i \end{cases};$$

$i, j = \overline{1, I}, k, r = 1, 2, 3, l, p = 1, 2$ .

The remaining elements of matrices  $B^x$  and  $B^y$  are equal to zero.